Q. J. R. Meteorol. Soc. (2002), **128**, pp. 625–646

Aspects of the parametrization of organized convection: Contrasting cloud-resolving model and single-column model realizations

By D. GREGORY[1] and F. GUICHARD[2]*

[1]*European Centre for Medium-Range Weather Forecasts, UK*
[2]*CNRM-GAME (CNRS and Météo-France), France*

(Received 11 October 2000; revised 30 March 2001)

SUMMARY

Cloud-resolving model (CRM) simulations of organized tropical convection observed in the Tropical Ocean/Global Atmosphere Coupled Ocean–Atmosphere Response Experiment are used to evaluate versions of the European Centre for Medium-Range Weather Forecasts convection and cloud schemes in single-column model simulations. Emphasis is placed upon the ability of the convection scheme to represent 'convective-scale' processes with typically mode-1 heating structures through the troposphere, together with a cloud scheme representing the 'stratiform (mesoscale) component' with upper-level heating and low-level cooling due to the evaporation of precipitation. While diagnosis of convective and stratiform precipitation is sensitive to the sampling criteria applied to the CRM, vertical structures of the mass and heat budgets are robust. Using diagnostics from the CRM simulations as a guide, revisions to the convection and cloud schemes are suggested in order to enable the parametrization to represent the two scales. The study suggests that a mass-flux convection scheme linked via detrainment to a prognostic treatment of cloud can represent organized convection, provided that the upward motion in the upper-level stratiform cloud is considered.

KEYWORDS: GCSS General-circulation models Numerical weather prediction TOGA COARE

1. INTRODUCTION

The development of representations of convective processes for large-scale models has been a subject of importance to meteorologists for the past 40 years. Early large-scale models of the atmosphere tended to view the parametrization of convection as a mechanism for maintaining stability, through crude adjustments of the thermodynamic profile to moist neutrality. Observations of convection during the 1960s and 1970s led to the development of parametrizations (such as Kuo-type schemes (Kuo 1965) and the mass-flux approach pioneered by Arakawa and Schubert (1974)) based upon the insights obtained. Over the past ten years the mass-flux approach has come to dominate the field.

Key to many of these developments has been the use of observational data both to provide insight into convective processes and also to evaluate the performance of convection schemes in single-column model (SCM) simulations (Betts and Miller 1986; Tiedtke 1989; Gregory and Rowntree 1990). The most frequently used observational experiment in this regard has been GATE†. The TOGA COARE‡ now provides a more recent complementary dataset. A limitation of such data is that they only provide a view of the bulk effects of convection. For example mass-flux theory points to the importance of the convective mass flux in determining the intensity and vertical distribution of convective heating. This cannot be obtained directly from observations, although Yanai *et al.* (1973) demonstrated a technique to obtain such information from observations through a diagnostic application of mass-flux theory. This method has since been used by a number of workers studying deep and shallow convection. However, as a parametrization is used in its derivation, care must be exercised in the use of such data to evaluate and develop convection schemes.

* Corresponding author: CNRM-GAME (CNRS and Météo-France), 42 av Coriolis, 31057 Toulouse Cedex, France.

† GARP (Global Atmospheric Research Programme) Atlantic Tropical Experiment.

‡ Tropical Ocean/Global Atmosphere Coupled Ocean–Atmosphere Response Experiment.

Because of such limitations and uncertainties in the use of observational data, the possibility of using cloud-resolving models (CRMs) in the development of convection schemes has been considered for many years. Early attempts include work by Soong and Tao (1980), Krueger (1988) and Gregory and Miller (1989). Such work encouraged initiatives such as the GCSS* (see the paper by the GEWEX Cloud System Science Team (1993)) with its twin emphases of improving CRMs through comparison against observed cases and of using such simulations, together with more idealized ones, to aid the development of parametrizations for large-scale models. Although uncertainty remains as to how best to represent cloud microphysical processes, CRMs have been shown to capture the main interactions between dynamics and latent-heat release, as has been recently demonstrated by the study of a TOGA COARE squall line reported by Redelsperger *et al.* (2000), for example. Comparison of multi-day and multi-week simulations of convective systems in GATE and TOGA COARE in both two dimensions (Wu *et al.* 1998; Li *et al.* 1999; Guichard *et al.* 2000) and three dimensions (Grabowski *et al.* 1998) with observed characteristics of convection has added credibility to the use of CRM-derived data in assisting the development of parametrizations. For example Wu and Moncrieff (2001), by comparing a CRM and an SCM version of the third NCAR† Community Climate Model (CCM3) have inferred inadequacies in the latter's treatment of cloud–radiation interactions. Idealized experiments have also been used in the development of parametrizations. Gregory *et al.* (1997) developed a representation of convective momentum transports based upon CRM simulations of idealized tropical and cold-air-outbreak convection. However, as is demonstrated later in this paper, uncertainties remain in defining diagnostic quantities from CRMs to compare with parametrizations.

Traditionally, the convection scheme in a general-circulation model (GCM) is used to determine vertical fluxes of heat and moisture and, in some models, the momentum fluxes also. In the tropics of many GCMs, such schemes are responsible for the majority of the latent-heat release and surface precipitation. However, it is recognized that a significant proportion of the precipitation in convective cloud systems arises not from regions of rapid ascent, which most convection schemes aim to model, but from extensive layers of stratiform cloud which also have significant radiative impact. During GATE it was estimated that 30–40% of the surface precipitation originated not from regions of active convection but from extensive layers of stratiform clouds. In a study of cloud systems during TOGA COARE, Yuter and Houze (1998) estimated that, during the active phase of the intra-seasonal oscillation, 70% of the rain from cloud systems originated from extensive areas of stratiform cloud.

Johnson (1984) extended the method of Yanai *et al.* (1973) to incorporate a description of stratiform updraughts and downdraughts, attempting to gain insight into the properties of such clouds and their contribution to the net convective heating. Rather than the mode-1 structure of heating from deep convection, a mode-2 structure is associated with these stratiform features, with upper-level ascent and condensational heating above the freezing level and descent below, driven by the evaporation of precipitation and dynamical processes. These modes have different interactions with the larger-scale flow. Mapes (1996) pointed out that gravity waves forced by a mode-2 heating/cooling structure have a phase speed half that of gravity waves associated with mode-1 heating. As well as having potential impacts upon the evolution of flow patterns, the correct classification of precipitation in tropical cloud systems is likely to be important if

* GEWEX (Global Energy and Water-cycle EXperiment) Cloud Systems Study.

† National Center for Atmospheric Research.

precipitation data from satellites, such as the Tropical Rainfall Measurement Mission (TRMM), are to be correctly used within the context of data assimilation systems of numerical weather prediction (NWP). If precipitation associated with the mode-2 structure of stratiform regions is attributed to regions of active convection with a mode-1 heating structure, systematic errors may occur. For cloud systems over land, differences in the characteristics of convective-scale and stratiform-scale precipitation are likely to lead to different interactions with the surface hydrology. Stratiform precipitation is less intense than that from convective towers and so will be less prone to surface run-off.

The mesoscale stratiform component of convective cloud systems has received more attention in the mesoscale modelling community. There, it is recognized that, with horizontal resolutions of 20–30 km and with a link between sources of condensed water from a convection scheme and resolved model fields, the stratiform region of organized convective cloud systems can be successfully simulated (e.g. Zhang and Fritsh 1986). As noted previously, most GCMs continue to rely on their convection scheme alone to represent the effects of both the convective and stratiform regions. Donner (1993), Alexander and Cotton (1998) and Gray (2001) have all proposed parametrizations of these features based upon an extension of the mass-flux approach, similar to that first described by Johnson (1984). However, none of these has, as yet, been incorporated into a GCM. Here, an alternative methodology is evaluated that is more akin to that used within the mesoscale modelling community. Linked convection and cloud schemes are used to represent the active convection and stratiform regions, respectively.

This paper describes the use of CRM simulations to evaluate the ability of the convection and cloud schemes used in the ECMWF* model (a part of the Integrated Forecasting System (IFS) in use at ECMWF) to represent organized convective cloud systems. The CRM simulations are carried out using the CNRM† CRM. Both of the cloud systems considered were observed during TOGA COARE and, in each, both convective-scale and stratiform-scale motions were present. The first case is a squall line observed on 22 February 1993, while the second concerns convection in the Intensive Flux Array (IFA) between 20 and 26 December 1992. The cases are part of an intercomparison of CRMs and SCMs organized by GCSS Working Group 4 (deep precipitating convection) (Moncrieff *et al.* 1997). Redelsperger *et al.* (2000) and Krueger (1997) have described simulations carried out by several different CRMs for these cases, comparing the results with available observations. Bechtold *et al.* (2000) has also compared SCM simulations with both observations and data from CRM simulations for the first of these cases.

Unlike studies such as that of Wu and Moncrieff (2001), the focus here is not on the interaction of the parametrized clouds and radiation. Rather it is upon whether the contribution of the convection and cloud schemes are broadly reasonable in representing organized convective systems in SCM simulations. Both models are briefly described in section 2, together with revisions to the cloud and convection scheme that have resulted from this study. The performances of the control and revised schemes are contrasted in section 3. Although simulations from a single CRM are used to characterize convection in each case, the performance of the CNRM model is characteristic of the range of CRM simulations discussed by Redelsperger *et al.* (2000) and Krueger (1997). Moreover, it should be noted that the aim is for the parametrized description of the cloud system to broadly follow the CRM rather than match it exactly.

* European Centre for Medium-Range Weather Forecasts.

† Centre National de Recherches Météorologiques.

2. Description of the models

(*a*) *The CNRM mesoscale model*

The CRM of Redelsperger and Sommeria (1986) is used to simulate explicitly the convective systems. This is an anelastic non-hydrostatic model, which has already been extensively used for studying squall-line-type systems (Lafore *et al.* 1988; Redelsperger and Lafore 1988). The model prognostic variables are the horizontal and vertical winds, the potential temperature and the water-vapour mixing ratio. Five hydrometeor species (cloud liquid droplets, rain drops, ice crystals, aggregates and graupel) and the subgrid turbulent kinetic energy are also prognostic. A subgrid condensation scheme with a Kessler-type parametrization is used for warm microphysical processes (Redelsperger and Sommeria 1986). Ice-phase microphysical processes are handled by the scheme developed by Caniaux *et al.* (1994). Radiative effects are treated by the parametrization of Morcrette (1990), as described by Guichard *et al.* (1996), and the surface-flux treatment follows Louis (1979).

(*b*) *The ECMWF single-column model*

The SCM is based upon the atmospheric component of cycle CY13R4 of the ECMWF IFS, although modifications to the cloud and convection scheme have been made to bring the control version up to CY18R3 (Gregory *et al.* 2000). This version has been previously used in the study by Gregory (2001), and here uses the standard ECMWF 31 levels in the vertical. The effects of dynamical processes are incorporated through imposing prescribed heating/moistening rates from observations or CRMs, together with the large-scale vertical velocity. As in the CRM, the radiation parametrization of Morcrette (1990) is used. The moist convection and cloud schemes are considered in more detail below, being based upon those described by Tiedtke (1989, 1993). The vertical diffusion parametrization is based on K-theory, with a K-profile closure (Beljaars and Viterbo 1998) for the unstable boundary layer, a Richardson-number-dependent diffusion coefficient for stable situations above the surface layer (Viterbo *et al.* 1999), and a Monin–Obukhov type closure in the surface layer (Beljaars and Holtslag 1991).

(*c*) *Convection scheme*

The convection scheme used in the control SCM simulations, described by Gregory *et al.* (2000), is a development of the bulk mass-flux scheme of Tiedtke (1993). A CAPE*-adjustment closure is used for deep convection, the cloud-base mass flux being determined from the assumption that convection acts to reduce CAPE to zero over a specified timescale. As part of this study, further modifications were made to the entrainment/detrainment formulation, updraught cloud microphysical processes and downdraughts.

(i) *Entrainment and detrainment formulation.* As in the paper by Tiedtke (1989), the control scheme includes two types of entrainment and detrainment. 'Mixing entrainment and detrainment' represent the transfer of mass across the cloud boundary by turbulence, with entrainment and detrainment rates of 1×10^{-4} m^{-1} for deep convection and 3×10^{-4} m^{-1} for shallow convection. These values are increased in the lowest part of the convecting layer, by a factor of four at cloud base, decreasing linearly back to the constant values above 150 hPa. This attempts to reflect large-eddy model simulations which suggest the existence of larger lateral mixing rates in shallow convection.

* Convective Available Potential Energy.

For deep convection a second 'organized' entrainment flux is included, linked to the moisture convergence into a column of the atmosphere, allowing the updraught mass flux to grow with height;

$$\frac{\partial M_{\mathrm{UD}}}{\partial z} = -\frac{\overline{\rho}}{\overline{q}}\left(\overline{\mathbf{V}} \cdot \nabla \overline{q} + \overline{w}\frac{\partial \overline{q}}{\partial z}\right), \tag{1}$$

where M_{UD} is the updraught mass flux, q is the humidity mixing ratio, ρ is the density, $\mathbf{V}$ is the horizontal velocity and w is the vertical velocity. Overbars denote large-scale averages.

In the revised scheme both types of entrainment are replaced by the formulation derived by Gregory (2001), by considering the effect of entrainment upon the cloud kinetic energy budget;

$$\epsilon(\overline{w}^{\mathrm{UD}})^2 = C_\epsilon a g \overline{\left(\frac{T'_{\mathrm{v}}}{\overline{T}_{\mathrm{v}}} - l\right)}^{\mathrm{UD}}, \tag{2}$$

where the notation $\overline{\ }^{\mathrm{UD}}$ refers to updraught quantities, ϵ is the entrainment rate, T'_{v} is the excess virtual temperature of the updraught, $\overline{T}_{\mathrm{v}}$ is the large-scale virtual temperature and l is condensed water. C_ϵ is an entrainment coefficient set to 0.25, g is the acceleration of gravity, while a accounts for the effect of vertical pressure gradients upon the net buoyancy of a parcel, being set to 1/6 (see Gregory (2001) for further discussion of these parameters). The detrainment rate for deep convection is increased to 2×10^{-4} m^{-1}, corresponding to a decay height of 5 km for a convective plume if there were no entrainment.

(ii) *Updraught cloud microphysics and vertical velocity.* The control scheme includes a simple precipitation microphysics scheme, similar to that used in the cloud scheme of Tiedtke (1993), although accretion of cloud water by falling precipitation is not included. The timescale over which microphysical processes act is determined by the thickness of a model layer and the updraught vertical velocity is estimated by the approximate equation suggested by Simpson and Wiggert (1969).

The scheme is retained in the revised scheme, although the autoconversion coefficient is increased from 1×10^{-3} to 3×10^{-3} s^{-1} while the Bergeron–Findeison process is switched off. These changes are somewhat ad hoc and reflect the crudity of the microphysical treatment. However, they give better agreement with the CRM simulations, allowing more precipitation to fall from the updraught rather than being cycled through the cloud scheme via detrainment. Updraught vertical velocity is estimated from an alternative equation discussed by Gregory (2001). This is also used in estimating the updraught entrainment rate (Eq. (2)).

(iii) *Convective downdraughts.* Convective downdraughts are represented by an inverted entraining/detraining plume maintained at saturation during descent by evaporation of precipitation. In the standard scheme downdraughts are triggered from the highest level where an equal mixture of updraught and environment air brought to saturation is colder than the environment (the level of free sinking), with the initial mass flux set to 30% of the updraught mass flux at cloud base.

Both these assumptions are modified in the revised scheme. SCM tests during this study indicated that the need for an initial negative temperature excess led to intermittent triggering of the downdraught scheme. The criterion was relaxed to allow downdraughts to form when the initial mixture was colder than 1 K above the cloud environment

temperature; this leads to a more continuous response. In order to strengthen the link between deep convection and downdraught formation, the initial downdraught mass flux is related to the updraught mass flux at the level of free sinking, the proportionality factor of 0.3 being retained.

(*d*) *Cloud scheme*

The prognostic cloud scheme has been described in detail by Tiedtke (1993), changes to the treatment of ice fallout being documented by Gregory *et al.* (2000). It is based upon the conservation of cloudy mass and has two prognostic variables—liquid and ice water, and cloud fraction. Various processes are represented that allow the growth and decay of these quantities. Of importance to the cases discussed here is that the liquid and ice water, and the cloudy mass detrained from the convection scheme, are passed to the cloud scheme as sources of condensate and cloud area.

Cloud condensate and fraction also vary according to the environmental vertical motion,

$$w_e = \overline{w} - \frac{M_c}{\rho}, \tag{3}$$

the rate of change of both condensate and fraction being proportional to the change in saturation specific humidity with a time implied by w_e*. This assumes that, within a grid box, there is a distribution of specific humidity, with different portions becoming saturated as the mean temperature of a layer decreases. In the case of organized convection discussed here, this process plays a significant role in the net diabatic heating budget.

As it falls from cloud, precipitation evaporates within clear air. In the original version of the Tiedtke (1993) scheme, no evaporation was allowed in the presence of convection if the relative humidity in a layer was greater than 70%. Although rather arbitrary, this was introduced to prevent excessive humidities developing in the lower troposphere when the scheme was initially introduced into the ECMWF operational NWP model. In the revised SCM this has been relaxed to 80%. Sensitivity of the results to this parameter is large and is explored later.

3. Comparison of CRM and SCM realizations

The CRM and SCM simulations of two cases of organized tropical convection from TOGA COARE (Webster and Lukas 1992) have been compared.

(*a*) *The TOGA COARE 22 February squall line*

The case has been described in some detail by Redelsperger *et al.* (2000), being a squall-line-type system with a horizontal dimension of the order of 100 km oriented approximately south–north perpendicular to the low-level wind shear. Having a lifetime of several hours, the system propagated eastwards with a speed of more than 10 m s^{-1} and had a pronounced mesoscale organization typical of previously reported architypal structures (e.g. Zipser 1977). Doppler radar observations of the system showed strong convective updraughts at the leading edge of the system, with a maximum in the vertical velocity around 3–4 km. Towards the rear of the system, a second maximum of vertical

* In the original version of the scheme this term was only allowed to operate in the presence of convection if $w_e < 0$. Jakob *et al.* (1999) have discussed a relaxation of this criterion which has been included into recent versions of the operational model at ECMWF.

velocity is present, located at higher levels than for the convective updraught, with subsidence below.

(i) *Cloud-resolving model realizations.* The experimental design for the CRM simulation was as discussed by Redelsperger *et al.* (2000). The simulation was performed over a three-dimensional domain, having a dimension of 100 km in the zonal direction, 125 km in the meridional direction, and a horizontal resolution of 1.25 km. The domain height was 23 km with a variable-resolution vertical grid. Open lateral boundary conditions, suitable for this type of self-organized convective system were used, allowing the development of a mean vertical mass flux associated with the convective activity in the domain. Convection was initialized from a cold and dry bubble and the period of integration was seven hours, the storm reaching its mature stage after a few hours (although it continued to grow in magnitude throughout the simulation).

Redelsperger *et al.* (2000) showed that the structure of the cloud system, as revealed by Doppler radar observations, is fairly well captured in the CRM simulation. Here, the focus is upon describing the mean structure of the convective and stratiform components of the system in order to assess the ability of the parametrized cloud and convection schemes to represent such a system. Several authors (e.g. Tao and Simpson 1989; Xu 1995) have suggested sampling techniques by which the mean properties of convective and stratiform regions of mesoscale cloud systems can be isolated from the CRM simulations. Here, following Guichard *et al.* (1997), convective and stratiform regions of the domain are isolated through sampling based upon surface precipitation rate and cloud water content. A column is defined as being convective if the surface precipitation rate is greater than 20 mm h^{-1}, or greater than 4 mm h^{-1} and twice as large than the mean precipitation rate over the 24 surrounding grids points. In the latter case the closest eight grids points are also counted as convective columns. An additional criterion is added to this previously used methodology in order to capture convective cells that are not yet precipitating; if cloud water at any level within a column below the freezing level exceeds 0.5 g kg^{-1} the column is considered to be convective. The remaining columns in which liquid water or ice contents exceed 5×10^{-3} g kg^{-1} are counted as being stratiform. The sensitivity of the diagnosed properties of convective and stratiform regions to the sampling criteria is discussed in section 3(b) when considering a second case of organized convection.

Although uncertainty exists, the criteria described appear to partition the system successfully into areas of a convective or stratiform 'nature', as illustrated in vertical profiles of mass fluxes averaged over the three last hours of the simulation (Fig. 1(a)). The domain-averaged convective and stratiform mass fluxes are typical of an organized convective system (e.g. Leary and Houze 1980), both playing significant roles in determining the domain-mean mass flux. The convective region occupies of the order of 10% of the domain, and is composed almost entirely of intense convective cells located at the front of the system. Although its area is small, this region is responsible for all of the ascent in the lower troposphere, the peak convective mass flux near 3 km indicating, in terms of a plume description of the convective updraught, large entrainment rates below this level. The convective mass flux decreases above 6 km, indicating net detrainment of air above this level. The contribution from the stratiform part of the system is also significant with upper-level ascent and low-level descent. Motion within clear air contributes a smaller amount to the domain-mean mass flux, but is comparable in magnitude to that seen in convective regions in the upper troposphere, although of opposite sign.

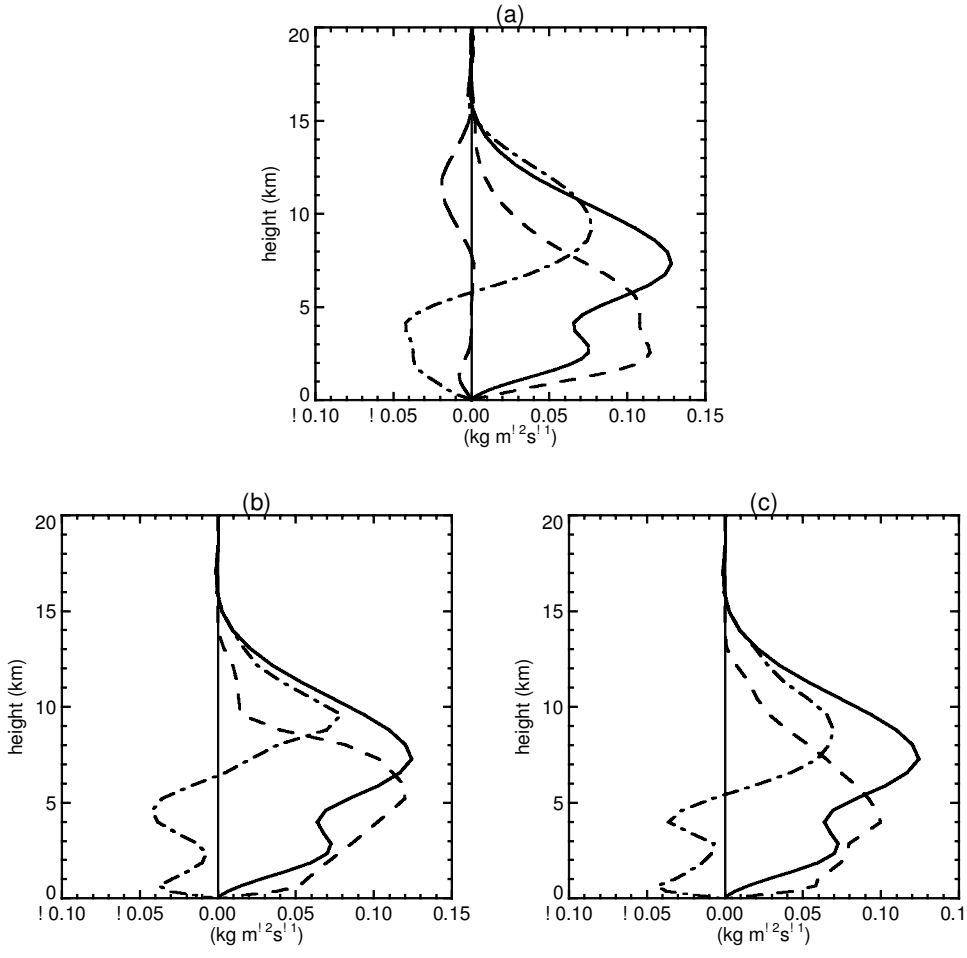

Figure 1. Partition of the total mass flux (solid lines) into convective (short-dashed lines), stratiform (dot-dashed lines) and clear-sky-environmen t (long-dashed line) mass fluxes averaged over the period 4–7 hours from (a) the cloud-resolving model, (b) the standard single-column model, and (c) the revised single-column model.

(ii) *Single-column model realizations.* The SCM simulations follow the methodology discussed by Bechtold *et al.* (2000) in which several SCM simulations of the case are compared with data from CRM simulation. No observationally based large-scale forcing tendencies are available for the case, and so the domain-average vertical velocity and tendencies of temperature and humidity due to horizontal and vertical advection are calculated from the CRM simulation and used to force the SCM. Specific details of the large-scale forcing can be found in the paper by Bechtold *et al.* (2000) but, as the large-scale forcing is dominated by vertical advection, the vertical structure may be inferred from that of the total mass flux in Figs. 1(a)–(c). It should be noted that the forcing provided to the SCM is driven purely by the internal circulation of the CRM simulation, and so may not match similar quantities which might have been derived if sufficient sounding data were available. However, their use in the SCM simulations allows the bulk evolution of the SCM and CRM simulations to be comparable. The maximum intensity of the temperature forcing provided to the SCM is -80 K day^{-1}. To allow convection to respond adequately to such a large forcing, a time step of 5 min and an

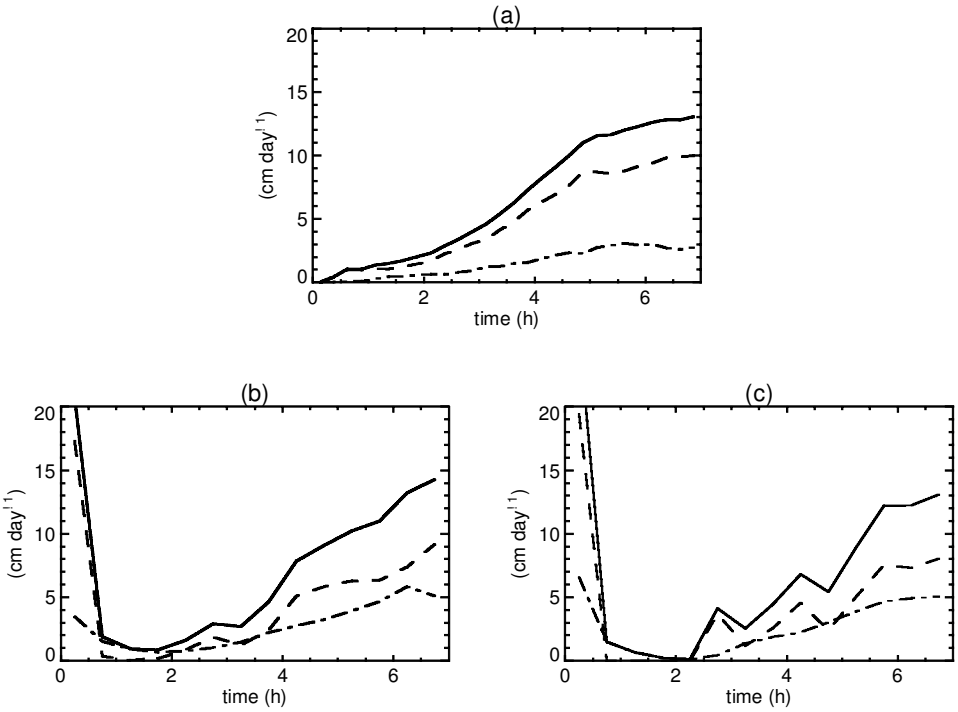

Figure 2. Time-series of 30 min average total precipitation (solid lines), convective precipitation (dashed lines) and stratiform precipitation (dot-dashed lines) from (a) the cloud-resolving model, (b) the standard single-column model, and (c) revised single-column model.

adjustment timescale of 30 min are used, typical of that used in T213 versions of the ECMWF operational model (Gregory *et al.* 2000).

In comparing the SCM simulations with the CRM realization, the assumption is made that the convection scheme aims to represent convective-scale processes while the cloud scheme accounts for processes within the stratiform region of the cloud system. Although this would appear to be reasonable, as discussed in the introduction it is different from previous views of convection parametrization, where the thermodynamics of both convective and stratiform regions have been represented by the convection scheme alone. Figure 2(a) shows the time-series of the precipitation from the CRM simulation. The total precipitation gradually increases up to 12 cm day^{-1} at the end of the simulation. During the last three hours of the simulation, when the squall line is in a mature phase, the stratiform precipitation contributes approximately 20% of the total, a value typical of that found over a wide range of linear mesoscale convective systems seen in TOGA COARE (Rickenbach and Rutledge 1998). Both SCM simulations, using the control and the revised convection schemes, capture the broad evolution of the surface precipitation, as indeed they must as the physics of the model comes into balance with the imposed large-scale forcing from the CRM. In contrast to the gradual growth of precipitation in the CRM, the SCM simulations have large precipitation rates during the first hour due to the large amount of instability present within the initial profiles (CAPE exceeding 1500 J kg^{-1}). There is no inbuilt delay within the convection scheme to allow for the gradual development of convective cells, as in the CRM simulations. However, after the second hour, when the system is mature, the growth of the precipitation in

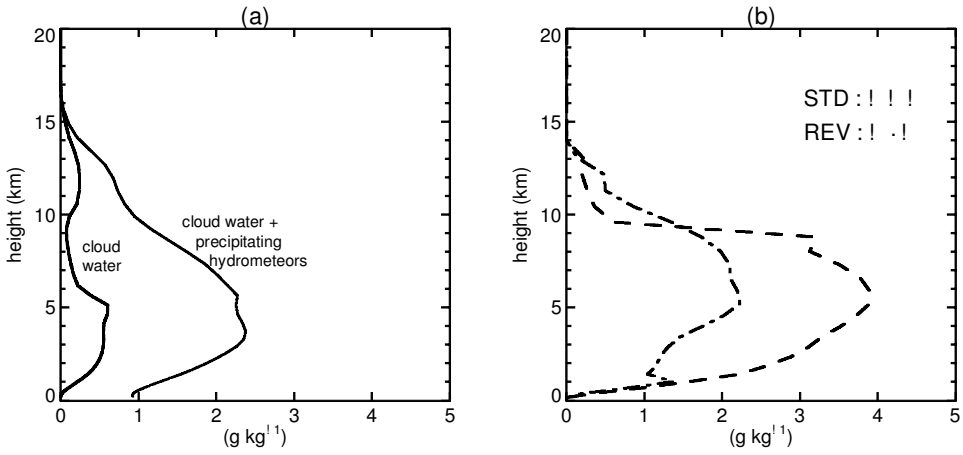

Figure 3. Vertical profiles of (a) the convective updraught (with $w > 1$ m s^{-1} only) cloud water (thick solid line) and the total cloud water (including hydrometeors) (thin solid line) from the cloud-resolving model averaged over the period 4–7 hours, and (b) the updraught condensate mixing ratio from the standard single-column model (dashed line) and the revised single-column model (dot-dashed line).

the SCM is comparable with that in the CRM. Averaging between four and seven hours, 70% of the surface precipitation originates directly from the convection scheme with the revised scheme, compared with 60% with the standard scheme. In the CRM simulation, 80% of the surface precipitation was diagnosed as being convective in origin.

The mass-flux budget of the SCMs provides an insight into how the split in the surface precipitation between the cloud and convection schemes originates (Figs. 1(b) and (c)). Firstly, considering the control simulation during the final three hours of the simulation, the convective mass flux (updraught plus downdraught, although the latter is negligible during this last part of the simulations) peaks at 6 km, with a rapid decrease above this. Convection only penetrates above 10 km during the final hour of the simulation.

The large detrainment of mass from convection at heights between 6 and 9 km results from several factors. Linking the updraught entrainment rate to moisture convergence leads to strong dilution of the parcel. Water loading due to cloud water in the updraught also contributes. Updraught vertical velocities peak at over 5 m s^{-1} between 4 and 7 km, compared with 3 m s^{-1} (at 5 km) in the CRM for the stronger ones ($w > 1$ m s^{-1}). This excess vertical velocity limits the timescale over which microphysical processes act, although the values of the microphysical coefficients also play a significant role in determining the updraught water content. Comparison of updraught cloud water from the SCM and CRM simulations is complicated by the presence of falling precipitation in the CRM simulations. In the convection scheme, precipitation is assumed to fall to the ground within the timestep it forms. Figure 3(a) shows the updraught cloud water and total condensate (cloud plus falling and non-falling precipitation) from the CRM. It is clear that the control scheme (Fig. 3(b)) overestimates the updraught condensed water throughout the convection layer.

The difference between the convective mass flux and the imposed large-scale vertical velocity results in a significant environmental motion, as defined by Eq. (3). This has a mode-2 structure, with ascent above 6 km and descent below, comparable with the mass flux associated with the stratiform part of the cloud system in the CRM (Fig. 1(a)).

The term 'stratiform mass flux' is used to refer to this residual quantity although it is not identical to that diagnosed from the CRM, mostly because of differences in the convective mass flux. As discussed previously, this residual mass flux generates cloud water/mass within the cloud scheme of the SCM causing heating in the upper troposphere and cooling below.

Although the stratiform mass flux in the SCM simulation has a similar vertical structure to that in the CRM, between 5 and 9 km its magnitude is reduced, due to overestimation of the convective mass flux. Around 40% of the surface precipitation from the cloud scheme arises directly from condensation in the cloud scheme caused by the stratiform mass flux; the remainder results from the detrainment of condensate from the convective updraught. Even with the stratiform mass flux being lower than in the CRM, the fraction of precipitation that is stratiform is overestimated in the SCM. Excessive updraught water contents detrained into the cloud scheme, together with no evaporation of falling precipitation as the relative humidity of the lower troposphere exceeds the 70% threshold, contribute to this. Allowing precipitation to evaporate at all humidities decreases the contribution of stratiform precipitation to 30%. However, the structure of the mass-flux profiles remains similar.

Returning to the SCM simulation with the revised cloud and convection scheme, Fig. 1(c) shows that the mass budget over the final three hours of the simulation is in better agreement with that of the CRM than for the control version of the SCM. The depth of convection is more consistent through this period, the entrainment rate predicted from the updraught vertical kinetic energy being half of that of the original formulation, resulting in less dilution of the parcel. Convective mass flux increases gradually from the surface to a peak at 4 km, gradually reducing above this as detrainment becomes dominant. The height of the peak mass flux is higher than in the CRM (2 km), which may be due to overestimation of the intensity of convective downdraughts by the parametrization which are active throughout the averaging period. The updraught mass flux predicted by the parametrization peaks at around 1 km (with a magnitude of 0.18 kg $m^{-2}s^{-1}$), but this is offset by a low-level peak in the downdraught mass flux.

Modification of the updraught microphysics results in more reasonable updraught water and ice contents (Fig. 3(b)), also aided by lower updraught vertical velocities which peak at 7 km with a magnitude of 4.5 m s^{-1}, still higher and larger than those in the CRM (5 km and 3 m s^{-1}) but weaker than predicted by the original formulation. With increased stratiform mass flux, condensation in the cloud scheme in the upper troposphere is double that of the control scheme. Evaporation of falling precipitation below 5 km, due to relaxation of the critical relative humidity for evaporation, means that increased condensation does not result in larger amounts of stratiform precipitation. Overall the revisions to the cloud and convection schemes allow them to provide a more realistic representation of the cloud system.

Sensitivity to the convective-adjustment timescale was considered by repeating the simulations with a two-hour timescale. Although this four-fold increase should result in a decrease in convective mass flux of a similar magnitude, in the last three hours of the simulation only a 50% reduction is seen. This smaller sensitivity results from a doubling of CAPE through a warmer moister boundary layer. With a lower convective mass flux, the stratiform mass flux increases, and around 60% of the surface precipitation is stratiform in nature, compared with 40% and 30% for the control and the revised schemes with a shorter adjustment timescale. This sensitivity is larger than that found by Gregory *et al.* (2000) for changes of adjustment timescale in T63 seasonal simulations with the ECMWF IFS.

Above cloud base, the temperature profile is similar to the one in the simulations using a 30 min adjustment timescale, although the humidity profile is drier above 5 km by 0.25 g kg^{-1}. The lack of sensitivity in the temperature profile of the free troposphere results from condensational heating being the dominant component of the apparent heat source $Q1$, while vertical eddy transport due to convection plays a large role in determining the net effect of diabatic processes on the moisture field (represented by the latent-heat flux divergence $Q2$). With a longer convective-adjustment scale and weaker convective activity, increased condensation in the prognostic cloud scheme results in the net condensational heating and surface precipitation being unaffected. However, the cloud scheme has no representation of the vertical transport of moisture, leading to a larger sensitivity in the humidity structure. This may be a potential weakness of using the cloud scheme to represent the stratiform cloud compared with the mass-flux approach suggested by Donner (1993) and others.

(*b*) *Convection over the TOGA COARE intensive flux array, 20–26 December 1992*

This second case has been described by Krueger (1997) and has been the focus of simulations by several CRMs and SCMs, being the second intercomparison case of the GCSS working group 4. Several convective episodes of varying degrees of intensity occurred during this six-day period. Convection was less well organized than for the squall-line case, although the systems had a substantial mesoscale component. The models were initialized with the average IFA 00 UTC temperature, humidity and wind sounding on 20 December. Temperature and moisture tendencies due to horizontal and vertical advection derived by budget techniques from the TOGA COARE IFA sounding network (Lin and Johnson 1996) were given to both the models. Similarly derived vertical velocity profiles were additionally supplied to the SCM. For both models, the horizontal winds were adjusted back to observed values on a two-hour timescale. Surface fluxes are predicted by the models' surface schemes. Peak cooling rates due to large-scale forcing are near -40 K day^{-1}. A convective-adjustment timescale of two hours is used in the SCM simulations with a time step of 15 min. The size of the IFA over which the forcing is calculated is larger than for the previous case, and so a longer adjustment timescale is appropriate (Gregory *et al.* 2000). Using a 30 min adjustment timescale (as in the previous case) leads to intermittency of the convection scheme. Due to the length of integration it was necessary to use a two-dimensional version of the CNRM CRM with a domain of 256 km and a horizontal resolution of 2 km with which the performance of the control and revised physics in SCM simulations are contrasted.

To obtain estimates of quantities associated with convective and stratiform regions from the CRM simulations, three different sampling methodologies have been used. The first is that of Guichard *et al.* (1997) (referred as GLR97 hereafter) described in the previous section. Changes have been made to account for the two-dimensional geometry of the model. A column is defined as convective if the surface precipitation is greater than 20 mm h^{-1}, or greater than 4 mm h^{-1} and twice as large as the surrounding four columns. In the latter case the surrounding two columns are also considered to be convective. The additional criterion to account for non-precipitating convective cells used in case 1 above is not included here. The second is that described in Krueger *et al.* (1996) (referred to as CA296 hereafter), being based upon surface precipitation but with different criteria and averaging to define the convective columns—namely, surface precipitation exceeding 10 mm h^{-1}, or twice as large as the surrounding ten columns. A number of additional columns are added surrounding these 'core' convective columns depending upon the intensity of surface precipitation. The third methodology (XU95),

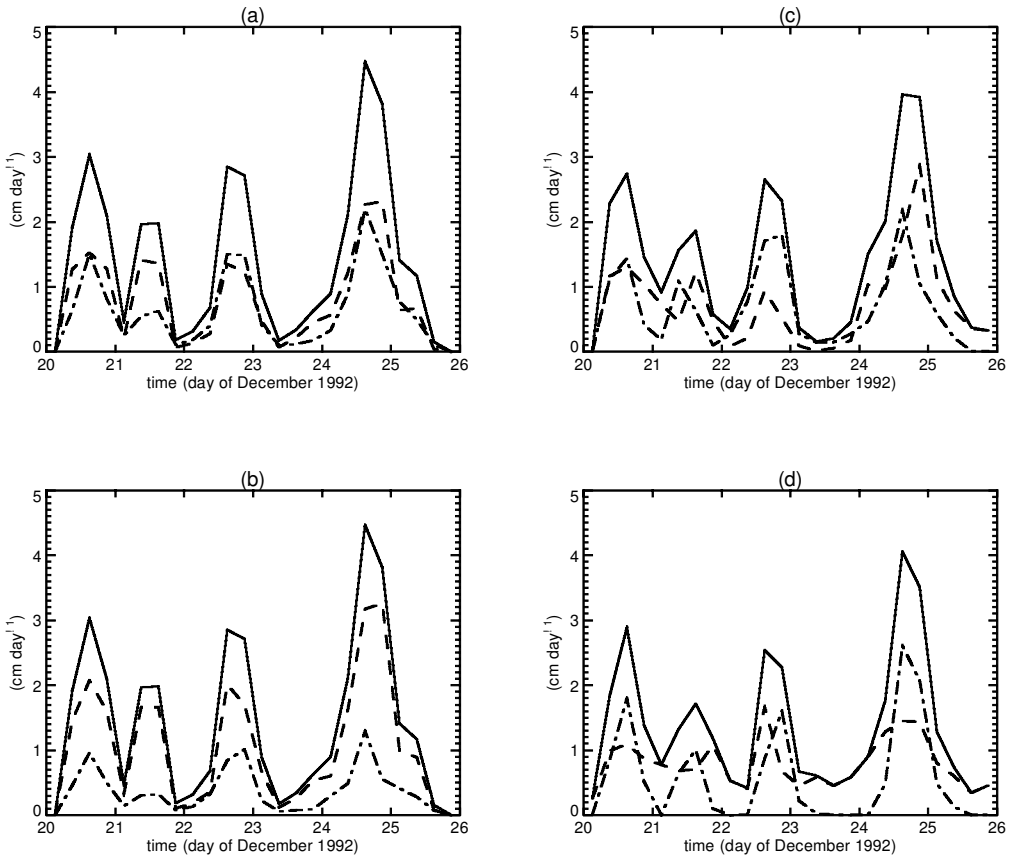

Figure 4. The time-series of the six-hour mean total precipitation (solid lines), convective precipitation (dashed lines), and stratiform precipitation (dot-dashed lines) from the cloud-resolving model partitioned with (a) the GLR97 and (b) the CA296 criteria (see text). Panels (c) and (d) are the same as (a) except that they are from the standard and the revised single-column models, respectively.

based upon vertical variations of the updraught vertical velocity, was proposed by Xu (1995) and is more suited for capturing convective cells that are not yet precipitating.

The split of total precipitation into convective and stratiform components is very sensitive to these criteria. Using either the GLR97 (Fig. 4(a)) or the XU95 (not shown) method, convective precipitation accounts for 50% of the total, while CA296 suggests that 75% of the total precipitation is convective (Fig. 4(b)). This difference is also reflected in the convection and stratiform contribution to $Q1$ (Figs. 5(a)–(d)). With the GLR97 criteria (Figs. 5(a) and (b)) the heating associated with the convective regions have a mode-1 structure in the vertical with the maximum heating in all events at 4 km. Heating in the stratiform regions is restricted to being above 4 km, the peak values being larger than those of the convective regions above this height. Cooling is found below 4 km associated with the evaporation of precipitation. With the CA296 criteria (Figs. 5(c) and (d)) a similar picture emerges, but the magnitude of the stratiform heating/cooling couplet is reduced, especially the heating component in the upper troposphere. While the maximum in convective heating remains near 4 km, the convective heating above this level is increased. This, together with the larger convective precipitation, shows that the CA296 criteria define more of the cloud within

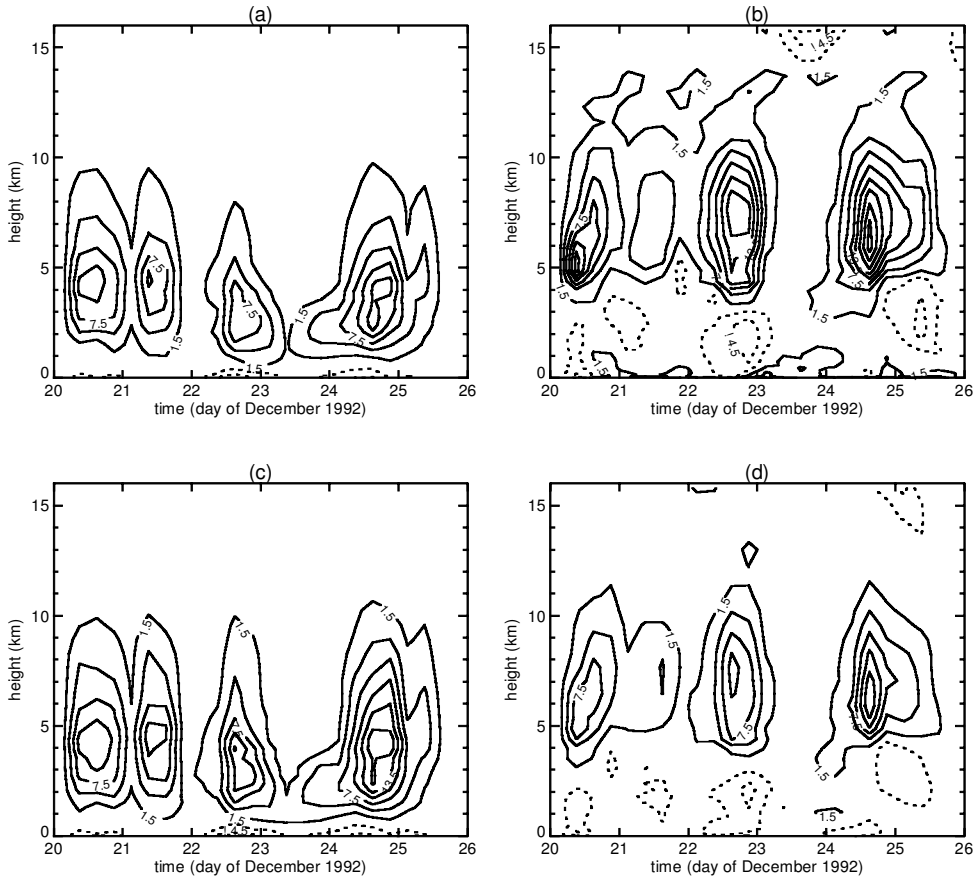

Figure 5. The temporal evolution of the six-hour (a) convective and (b) stratiform apparent heat source $Q1$ from the cloud-resolving model partitioned with the GLR97 criteria. Panels (c) and (d) are the same as (a) and (b), except that they are produced with the CA296 criteria. Panels (e) and (f) and panels (g) and (h) are the same as (a) and (b), except that they are produced from the standard and revised single-column models, respectively. The contour interval is 3 K day^{-1}, with negative contours dashed. See text for further information.

the simulation as being convective in nature, probably a consequence of the wider area around high precipitation regions included into the definition of convective columns. In addition, unlike the GLR97 method only the columns where precipitation occurs at the surface are counted as stratiform with the CA296 method, which also significantly reduces the magnitude of the upper-level stratiform heating.

Given the large variations in the characterizations of cloud systems in terms of convective and stratiform components of surface precipitation, it is difficult to distinguish using this alone whether the control or revised cloud and convection schemes provides a better description of cloud systems (Fig. 4(c) and (d)). With the control SCM, over the six-day period 55% of the total precipitation originates from the convection scheme, compared with 60% with the revised SCM. The temporal signature of the precipitation series is different. With the control SCM, peaks in stratiform precipitation often precede maxima in convective precipitation (21 and 24 December). With the revised scheme, peaks in convective precipitation precede, or are simultaneous with, peaks in stratiform precipitation. Stratiform precipitation dominates on 20 and 24 December, while convective activity is larger than in the CRM during suppressed periods. Comparison

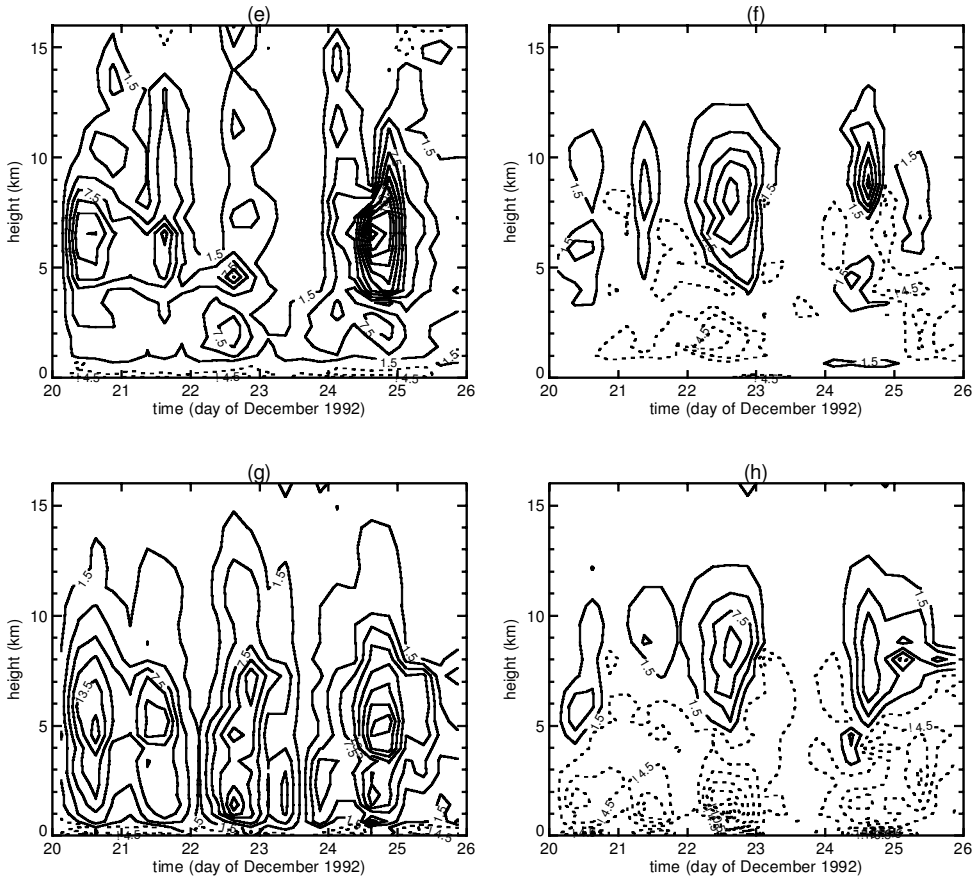

Figure 5. Continued.

of the mass fluxes in the SCM simulations with those associated with each region of the CRM (Fig. 6) provides further insight. For the CRM, using the GLR97 criteria, the convective-updraught mass flux peaks at 3 km, with a rapid decline above 4 km (Fig. 6(a)). The stratiform mass flux is almost as large as the updraught mass flux in the upper part of the cloud while convective downdraughts are stronger than the stratiform downdraught in the lower troposphere. The CA296 criteria give similar vertical structures, although above 5 km the convective mass is slightly larger and the stratiform mass is flux smaller, consistent with the previous analysis of $Q1$. In contrast, with the XU95 criteria one diagnoses a different structure of the convective-updraught mass flux below 5 km (Fig. 6(b)), with a larger maximum value peaking at a lower height and a vertical structure very similar to the one found with the modified GLR97 criteria for the squall-line case in section 3 (Fig. 1(a)). This is consistent with both criteria taking into account convective cells that are not generating precipitation at the surface. As a result, the net stratiform mass flux becomes negative from 4 km down to the surface, while above this height its magnitude is slightly weaker than with GLR97.

With the control SCM (Fig. 6(c)), the mass-flux profiles are in poor agreement with those in the CRM results, the peak convective-updraught mass flux being weaker and showing a smoother variation in height throughout the depth of the troposphere.

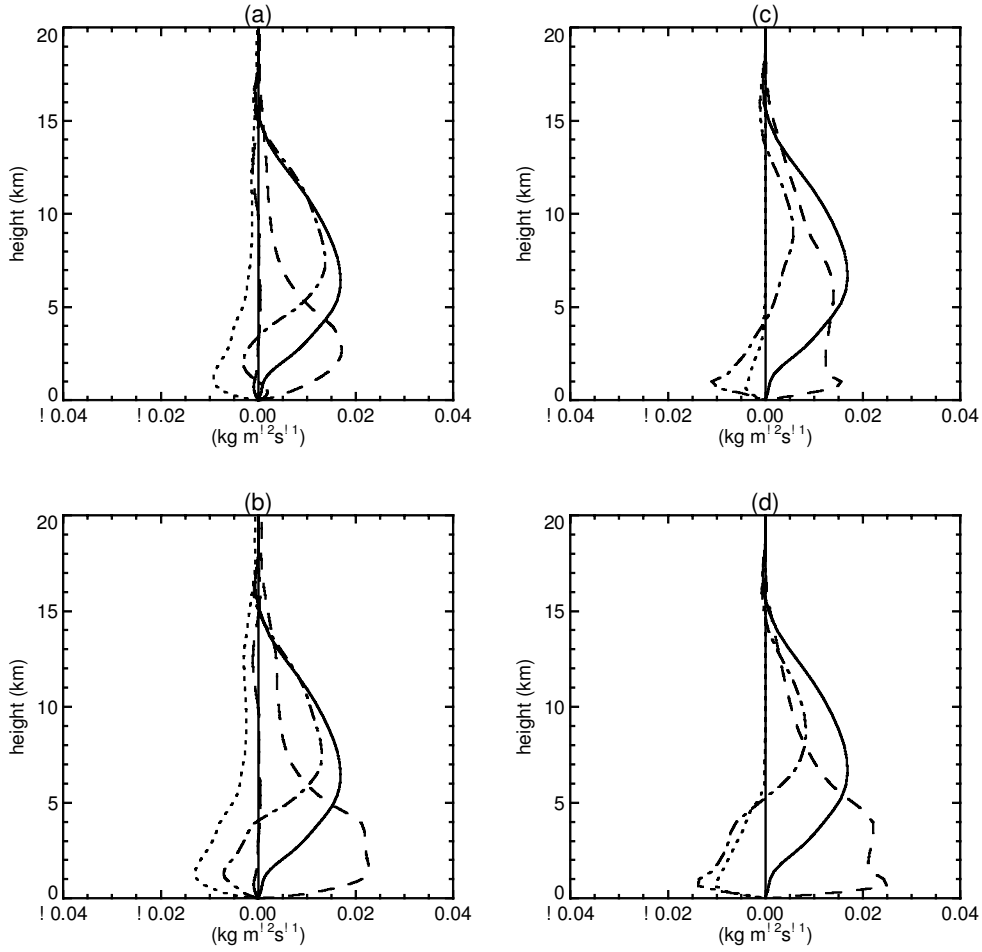

Figure 6. Partition of the total mass flux (solid lines) into convective updraught (short-dashed lines), convective downdraught (dotted lines), stratiform (dot-dashed lines) and clear-sky environment (long-dashed lines) mass fluxes averaged over the six-day period from the cloud-resolving model with (a) the GLR97 criteria and (b) the XU95 criteria (see text) for the convective area. Panels (c) and (d) are the same as (a), except they are from the standard and revised single-column models, respectively.

Stratiform mass fluxes are less than the updraught mass flux and much smaller than in the CRM. With the revised cloud and convection schemes (Fig. 6(d)) (as for the squall-line case above) the shape of the convective-updraught mass flux is in better agreement with that from the CRM. Indeed, the convective-updraught flux predicted by the revised SCM is close, both in terms of magnitude and structure, to the one obtained by the XU95 criteria (Fig. 6(b)). The decrease of updraught mass flux with height is less than in the CRM and the peak stratiform mass flux is underestimated by 30%. In the lower troposphere, convective downdraught mass fluxes are larger than in the standard scheme and in better agreement with the CRM, independently of the criteria used to define this quantity.

The improved representation of the cloud system by the revised parametrizations is seen in the contributions of the convection and cloud schemes to $Q1$. For the standard SCM (Figs. 5(e) and (f)), the maximum convective heating is found above 5 km, as might be expected from the mass-flux profile considered earlier. Heating rates below this

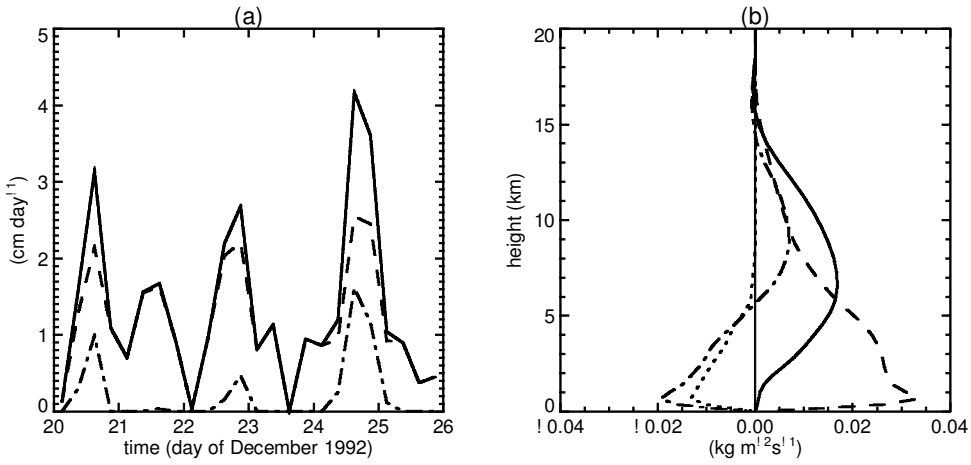

Figure 7. (a) As Fig. 4(d), and (b) as Fig. 6(d), except that the results were obtained from the revised single-column model with a relative-humidity threshold of $RH_c = 90\%$ instead of $RH_c = 80\%$.

are underestimated. Generally, heating from the cloud scheme in the upper troposphere is lower than that associated with the stratiform region of the CRM, although there is better agreement for the convective event on 22 December. While a large proportion of the surface precipitation originates from the cloud scheme, the condensational heating from this component of the model is nevertheless underestimated. This highlights the importance of the detrainment of condensed water from the convection scheme. Morcrette and Jakob (2000) found that, in seasonal simulations carried out with the ECMWF IFS at T63 using a convection scheme similar to the control version here, around 90% of the surface stratiform precipitation arises via detrainment from convection. While such a mechanism is realistic it plays a larger role than in the CRM simulation.

For the revised SCM simulation the shape of the convective heating profile (Fig. 5(g)) is in better agreement with that of the CRM. The variation in magnitude and depth is also better captured than is done by the standard schemes, although the level of the peak heating is slightly too high. The strongest convective heating is seen on 20 and 24 December, while weakest is on 21 December. On 22 December the CRM shows the depth of the convective heating decreasing through the event, with the heating greater than 3 K day^{-1} being restricted to below 5 km during the second half of the event. This is captured somewhat better with the revised convection scheme. While the heating due to the cloud scheme is increased above 5 km, the rates are still lower than diagnosed from the CRM.

Additional simulations were carried out to investigate sensitivities to the relative-humidity threshold used in the precipitation evaporation calculation and to the adjustment timescale of the CAPE adjustment closure of the convection scheme. Changing the former from 80% to 90% (Figs. 7(a) and (b)) reduces the stratiform precipitation over the six-day simulation from 40% to 15% (Fig. 7(a)). Convective precipitation is also reduced during the suppressed periods. While the structure of the mass flux remains similar (Fig. 7(b)), the peak updraught mass flux increases as the moistening of the lower troposphere leads to a larger CAPE. Increasing the adjustment timescale from two to eight hours (Figs. 8(a) and (b)) gives a reduction in the convective precipitation, from 60% to 45% for the revised schemes. The peak convective mass flux is only reduced by 20%, the change to the adjustment timescale being offset by an increase in CAPE due to

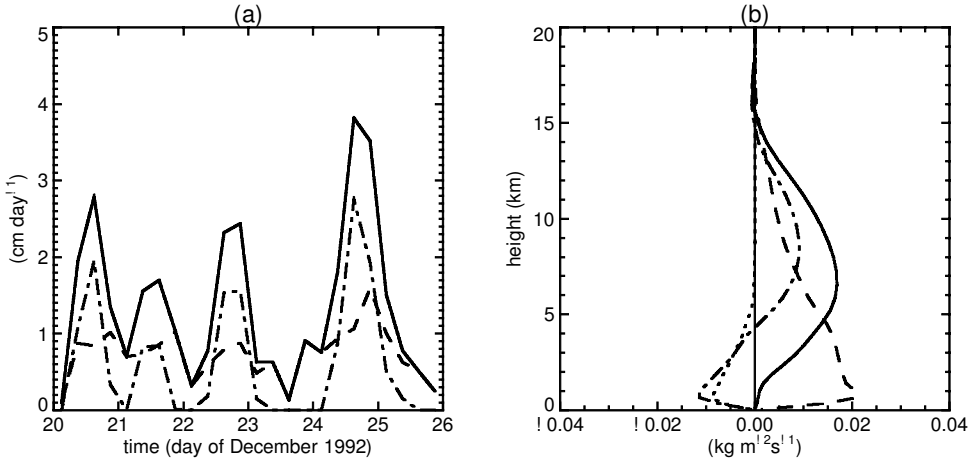

Figure 8. (a) As Fig. 4(d), and (b) as Fig. 6(d), except that the results were obtained from the revised single-column model with an adjustment timescale $\tau = 8$ hours instead of $\tau = 2$ hours.

a moister lower troposphere, as with the case above. However, the sensitivity indicated by this longer simulation to adjustment timescale is much less than found for the short squall-line simulation, being more typical of the sensitivity to the adjustment timescale found in seasonal simulations of the IFS (Gregory *et al.* 2000).

4. Further discussion

This paper has considered the representation of mesoscale convective systems in large-scale models. It has attempted to ask whether a combination of a mass-flux convection scheme with an explicit link via detrainment of condensate to a prognostic cloud scheme is a suitable vehicle to capture the main features of such systems. Comparison with CRM simulations of organized convection in the TOGA COARE suggests that this approach is reasonable and supports the revised view of the role of the convection and cloud schemes in the tropics, as discussed previously. Revision of the convective parametrization in light of comparison with CRM diagnostics improves the description of the mode-1 and mode-2 vertical structures of the convective and stratiform regions provided by each scheme. As with a number of previous studies (for example, Gregory *et al.* (1997) and Gregory (2001)), this demonstrates the utility of the use of CRMs to aid the development of improvements in parametrization, an aspect that has been encouraged over the recent years by the GCSS. However, a difficulty is the design of a robust characterization of which regions are convective and which are stratiform in the CRM, with different sampling criteria giving large variations in the split of mass fluxes between the two regions, and also in the surface precipitation attributed to them. This may cause difficulty in designing parametrizations for use in connection with the assimilation of convective and stratiform precipitation derived from satellite-borne radar in NWP data assimilation systems.

This study has not attempted to derive a full parametrization of the stratiform region. The SCM simulations were supplied with a mean vertical motion derived from either the CRM or from observations. From this, together with the convective mass flux, an estimate for the vertical motion within the stratiform part of the cloud system was obtained which was used to force the cloud scheme of the model. This is crucial to

the development of the stratiform cloud in the simulations here. In simulations with the revised SCM, around 50% of the condensed water within the upper-level cloud is due to condensation arising from vertical ascent as opposed to detrainment from the convection scheme. While, with resolutions of 20–30 km, the stratiform ascent might be explicitly resolved (Zhang and Fritsch 1986), in coarser-resolution models (such as those used in seasonal forecasting or in climate-change prediction) it needs to be parametrized. Schemes suggested by Donner (1993) and Gray (2001) address this aspect of the problem using a mass-flux approach. However, neither of these attempt to predict the cloud fraction or the longevity of stratiform clouds once convection has ceased, both of which are represented by the technique described in this paper. A future step towards a more comprehensive parametrization might be the merger of ideas presented by these two strands of development. Without inclusion of the effects of the stratiform mass flux upon upper-level clouds, in low-resolution models the mechanisms by which these are produced are likely to be dominated by the detrainment of condensate from the convection scheme. To achieve satisfactory results, the adjustment of the convection scheme to compensate for this missing process may be necessary. However, several other issues also need to be addressed. Not all convective systems develop large stratiform components, and so a 'triggering' algorithm is required. Also, if the convection and cloud schemes are to be used at a variety of resolutions, scaling of the stratiform mass flux will be needed because it becomes explicitly resolved at higher resolutions.

While recognizing these deficiencies in the representation of the stratiform region in coarse-resolution models, initial tests of the revised convection and cloud scheme were carried out in a T63 version of the ECMWF IFS. Impacts mainly arise through the revision of the convection scheme, with increased updraught detrainment rates leading to increased cloudiness in the middle troposphere and a 50/50% split between convective and stratiform processes in the zonal-mean tropical precipitation, rather than a 70/30% split with the standard scheme (Gregory *et al.* 2000). However, if the detrainment rate of the control scheme is used (half that of the revised scheme), the split in precipitation reverts back to that obtained using the standard scheme. Convective mass flux in the middle and upper troposphere is sensitive to this parameter, and this leads to variations in the mass flux seen by the cloud scheme. Although the detrainment formulation is a topic for future work, improved treatments of tropical cirrus may result only from the inclusion of a parametrization of the stratiform mass flux.

ACKNOWLEDGEMENTS

The authors would like to thank Jean-Luc Redelsperger (CNRM) for supporting the visit of Françoise Guichard to the ECMWF to work on the initial version of the revised convection and cloud schemes, thereby facilitating the comparisons of the SCM and CRM simulations. We have appreciated stimulating discussions with colleagues from the GCSS Working Group 4 and the European Cloud-Resolving Model Project concerning the two case studies described in the paper. The authors also thank R. H. Johnson and his research group for making available their TOGA COARE large-scale dataset.

REFERENCES

Alexander, G. D. and Cotton, W. R. 1998 The use of cloud-resolving simulations of mesoscale convective systems to build a mesoscale parameterization scheme. *J. Atmos. Sci.*, **55,** 2137–2161

Arakawa, A. and Schubert, W. H. 1974 Interaction of a cumulus cloud ensemble with the large-scale environment: Part I. *J. Atmos. Sci.*, **31,** 674–701

Bechtold, P., Redelsperger, J.-L., Beau, I., Blackburn, M., Brinkop, S., Grandpeix, J.-Y., Grant, D., Gregory, D., Guichard, F., Hoff, C. and Ioannidou, E. 2000 A GCSS model intercomparison for a tropical squall line observed during TOGA COARE. II: Intercomparison of single-column models and a cloud-resolving model. *Q. J. R. Meteorol. Soc.*, **126,** 865–888

Beljaars, A. C. M and Holtslag, A. A. M. 1991 Flux parametrization over land surfaces for atmospheric models. *J. Appl. Meteorol.*, **30,** 327–341

Beljaars, A. C. M. and Viterbo, P. 1998 'The role of the boundary layer in a numerical weather prediction model'. Pp. 287–304 in *Clear and cloudy boundary layers*, Eds. A. A. M. Holtslag and P. G. Duynkerke, Royal Netherlands Academy of Arts and Science

Betts, A. K. and Miller, M. J. 1986 A new convective adjustment scheme. II: Single-column tests using GATE-wave, BOMEX, ATEX and arctic air-mass datasets. *Q. J. R. Meteorol. Soc.*, **112,** 693–709

Caniaux, G., Redelsperger, J.-L. and Lafore, J.-P. 1994 A numerical study of the stratiform region of a fast-moving squall line. Part I: General description and water and heat budgets. *J. Atmos. Sci.*, **51,** 2046–2074

Donner, L. J. 1993 A cumulus parameterization including mass fluxes, vertical momentum dynamics and mesoscale effects. *J. Atmos. Sci.*, **50,** 889–906

GEWEX Cloud System Science Team 1993 The GEWEX cloud system study (GCSS). *Bull. Am. Meteorol. Soc.*, **74,** 387–399

Grabowski, W. M., Wu, X. and Moncrieff, M. W. 1998 Cloud-resolving modelling of cloud systems during phase III of GATE. Part II: Effects of resolution and the third spatial dimension., *J. Atmos. Sci.*, **55,** 3264–3282

Gray, M. E. B. 2001 Characteristics of numerically simulated mesoscale convective systems and their application to parametrization. *J. Atmos. Sci.*, **57,** 3953–3970

Gregory, D. 2001 Estimation of entrainment rate in simple models of convective clouds. *Q. J. R. Meteorol. Soc.*, **127,** 53–72

Gregory, D. and Miller, M. J. 1989 A numerical study of the parametrization of deep tropical convection. *Q. J. R. Meteorol. Soc.*, **115,** 1209–1241

Gregory, D. and Rowntree, P. R. 1990 A mass flux convection scheme with representation of cloud ensemble characteristics and stability-dependent closure. *Mon. Weather Rev.*, **118,** 1483–1506

Gregory, D., Kershaw, R. and Inness, P. M. 1997 Parametrization of momentum transport by convection. II: Tests in single-column and general circulation models. *Q. J. R. Meteorol. Soc.*, **123,** 1153–1184

Gregory, D., Morcrette, J.-J., Jakob, C., Beljaars, A. M. and Stockdale, T. 2000 Revision of convection, radiation and cloud schemes in the ECMWF model. *Q. J. R. Meteorol. Soc.*, **126,** 1685–1710

Guichard, F., Redelsperger, J.-L. and Lafore, J.-P. 1996 The behaviour of a cloud ensemble in response to external forcings. *Q. J. R. Meteorol. Soc.*, **122,** 1043–1073

Guichard, F., Lafore, J.-P. and Redelsperger, J.-L. 1997 Thermodynamical impact and internal structure of a tropical convective cloud system. *Q. J. R. Meteorol. Soc.*, **123,** 2297–2324

Guichard, F., Redelsperger, J.-L. and Lafore, J.-P. 2000 Cloud-resolving simulation of convective activity during TOGA COARE: Sensitivity to external sources of uncertainties. *Q. J. R. Meteorol. Soc.*, **126,** 3067–3096

Jakob, C., Gregory, D. and Texeria, J. 1999 'A package of cloud and convection changes for CY21R3'. Research Department Memorandum, European Centre for Medium-Range Weather Forecasts, Shinfield Park, Reading, UK

Johnson, R. H. 1984 Partitioning tropical heat and moisture budgets into cumulus and mesoscale components: Implications for cumulus parameterization. *Mon. Weather Rev.*, **112,** 1590–1601

Krueger, S. K. 1997 'A GCSS intercomparison of cloud-resolving models based on TOGA COARE observations'. Pp. 113–127 in Proceedings of the workshop on new insights and approaches to convective parameterization, 4–7 Nov 1997. European Centre for Medium-Range Weather Forecasts, Shinfield Park, Reading, UK

1988 Numerical simulation of tropical cumulus clouds and their interactions with the subcloud layer. *J. Atmos. Sci.*, **45,** 2221–2250

Krueger, S. K., Gregory, D., Moncrieff, M. W., Redelsperger, J.-L. and Tao, W.-K. 1996 'GCSS Working Group 4: First cloud-resolving model intercomparison project. Case 2'. Unpublished technical report, (available at http://www.met.utah.edu/skrueger/gcss / case2submit.html)

Kuo, H. L. 1965 On formation and intensification of tropical cyclones through latent heat release by cumulus convection. *J. Atmos. Sci.*, **22,** 40–62

Lafore, J.-P., Redelsperger, J.-L. and Jaubert, G. 1988 Comparison between a three-dimensional simulation and Doppler radar data of a tropical squall line: Transport of mass, momentum, heat and moisture. *J. Atmos. Sci.*, **45,** 3483–3500

Leary, C. A. and Houze, R. A. 1980 The contribution of mesoscale motions to the mass and heat fluxes of an intense tropical convective system. *J. Atmos. Sci.*, **37,** 784–796

Li, X., Sui, C.-H., Lau, K.-M. and Chou M.-D. 1999 Large-scale forcing and cloud–radiation interaction in the tropical deep convection regime. *J. Atmos. Sci.*, **56,** 3028–3042

Lin, X. and Johnson, R. H. 1996 Heating, moistening and rainfall over the western Pacific warm pool during TOGA COARE. *J. Atmos. Sci.*, **53,** 3367–3383

Louis, J. F. 1979 A parametric model of vertical eddy fluxes in the atmosphere. *Boundary-Layer Meteorol.*, **17,** 187–202

Mapes, B. 1996 'Mutual adjustment of mass flux and stratification profiles'. In *The physics and parametrization of moist atmospheric convection*, NATO ASI Series, Ed. R. K. Smith, Kluwer

Moncrieff, M. W., Krueger, S. K., Gregory, D., Redelsperger, J.-L. and Tao, W.-K. 1997 GEWEX Cloud System Study (GCSS) working group 4: Precipitating convective cloud systems. *Bull. Am. Meteorol. Soc.*, **78,** 831–844

Morcrette, J.-J. 1990 Impact of changes in the radiation transfer parametrization plus cloud optical properties in the ECMWF model. *Mon. Weather Rev.*, **118,** 847–873

Morcrette, J,-J. and Jakob, C. 2000 The response of the ECMWF model to changes in the cloud overlap assumption. *Mon. Weather Rev.,* **128,** 1707–1732

Redelsperger, J.-L. and Lafore, J.-P 1988 A three-dimensional simulation of a tropical squall line: Convective organization and thermodynamical transport. *J. Atmos. Sci.*, **45,** 1334–1356

Redelsperger, J.-L. and Sommeria, G. 1986 Three-dimensional simulation of a convective storm: Sensitivity studies on subgrid parameterization and spatial resolution. *J. Atmos. Sci.*, **43,** 2619–2635

Redelsperger, J.-L., Brown, P. R. A., Hoff, C., Guichard, F., Kawasima, M., Lang, S., Montmerle, T., Nakamura, K., Saito, K., Seman, C., Tao, W.-K. and Donner, L. J. 2000 A GCSS model intercomparison for a tropical squall line observed during TOGA COARE. I: Cloud-resolving models large-scale models. *Q. J. R. Meteorol. Soc.*, **126,** 823–864

Rickenbach, T. M. and Rutledge, S. A. 1998 Convection in TOGA COARE: Horizontal scale, morphology, and rainfall production. *J. Atmos. Sci.*, **55,** 2715–2729

Simpson, J. and Wiggert, V. 1969 Models of precipitating cumulus towers. *Mon. Weather Rev.*, **97,** 471–489

Soong, S.-T and Tao, W.-K. 1980 Response of deep tropical cumulus clouds to mesoscale processes. *J. Atmos. Sci.*, **37,** 2016–2034

Tao, W. K. and Simspon, J. 1989 Modeling study of a tropical squall-type convective line. *J. Atmos. Sci.*, **46,** 177–202

Tiedtke, M. 1989 A comprehensive mass flux scheme for cumulus parameterization in large-scale models. *Mon. Weather Rev.*, **117,** 1779–1800

1993 Representation of clouds in large-scale models. *Mon. Weather Rev.*, **121,** 3040–3061

Viterbo, P., Beljaars, A., Mahfouf, J.-F. and Teixeira, J. 1999 The representation of soil moisture freezing and its impact on the stable boundary layer. *Q. J. R. Meteorol. Soc.*, **125,** 2401–2426

Webster, P. J. and Lukas, R. 1992 TOGA COARE: The coupled ocean–atmosphere response experiment. *Bull. Am. Meteorol. Soc.*, **73,** 1377–1416

Wu, X. and Moncrieff, M. W. 2001 Long-term behaviour of cloud systems in TOGA COARE and their interaction with radiative and surface processes. Part III: Effects on the energy budget and SST. *J. Atmos. Sci.*, **58,** 1155–1168

Wu, X., Grabowski, W. W. and Moncrieff, M. W. 1998 Long-term behaviour of cloud systems in TOGA COARE and their interaction with radiative and surface processes. Part I: Two-dimensional modelling study. *J. Atmos. Sci.*, **55,** 2693–2714

Xu, K.-M. 1995 Partitioning mass, heat and moisture budgets of explicitly simulated cumulus ensembles into convective and stratiform components. *J. Atmos. Sci.*, **52,** 551–573

Yanai, M., Esbensen, S. and Chu, J.-H. 1973 Determination of bulk properties of tropical cloud clusters from large-scale heat and moisture budgets. *J. Atmos. Sci.*, **30,** 611–627

Yuter, S. E. and Houze Jr, R. A. 1998 The natural variability of precipitating clouds over the western Pacific warm pool. *Q. J. R. Meteorol. Soc.*, **124,** 53–100

Zhang, D.-L. and Fritsch, J.M. 1986 Numerical simulation of the meso-β-scale structure and evolution of the 1977 Johnstown flood. Part I: Model description and verification. *J. Atmos. Sci.*, **43,** 1913–1943

Zipser, E. 1977 Mesoscale and convective-scale downdrafts as distinct components of squall-line circulation. *Mon. Weather Rev.*, **105,** 1568–1589